Gli3-Deficient Mice Exhibit Cleft Palate Associated With Abnormal Tongue Development

Xi Huang,[1†] Steven L. Goudy,[2†] Tatiana Ketova,[1] Ying Litingtung,[1] and Chin Chiang[1*]

Palatogenesis depends on appropriate growth, elevation, and fusion of the palatal shelves and aberration in these processes can lead to palatal clefting. We observed a high incidence of palate clefting in mice deficient in Gli3, known for its role as a repressor in the absence of Shh signaling. In contrast with several current mouse models of cleft palate, Meckel's cartilage extension, cranial neural crest migration, palatal shelf proliferation, apoptosis, and key signaling components mediated by Shh, Bmp, Fgf, and Tgfβ, appeared unaffected in *Gli3*$^{-/-}$ mice. Palatal clefting in *Gli3*$^{-/-}$ mice was consistently associated with tongue abnormalities such as failure to flatten and improper positioning, implicating a critical role of Gli3 and normal tongue morphogenesis for timely palatal shelf elevation and joining. Furthermore, *Gli3*$^{-/-}$ palatal shelves grown in roller cultures without tongue can fuse suggesting that the abnormal tongue is likely an impediment for palatal shelf joining in *Gli3*$^{-/-}$ mutants. *Developmental Dynamics 237:3079–3087, 2008.*

Key words: Gli3 cleft palate tongue; cell proliferation; Shh

Accepted 29 July 2008

INTRODUCTION

Cleft palate is a congenital deformity resulting from the failure of palatal shelves to completely join. At an incidence of approximately 1 in 1,500 live births, cleft palate with or without cleft lip is one of the most common birth defects in humans (Stanier and Moore, 2004). Formation of the secondary palate involves coordinated outgrowth, elevation and fusion of the bilateral palatal shelves. In the mouse, these processes are initiated at embryonic day (E) 12 through bilateral outgrowths of the maxillary prominences, the primordial palatal shelves, along the wall of the anterior–posterior axis of the oropharynx. The palatal shelves then undergo transient vertical downward growth parallel to the lateral surface of the tongue. At E14, the shelves, facilitated by forward extension of the lower jaw, elevate above the tongue in a horizontal position where they contact and form the medial epithelial seam (MES) along the midline. The disappearance of MES at E15.5 results in the formation of a continuous palatal shelf (Stanier and Moore, 2004; Gritli-Linde, 2007).

The molecular mechanisms of palatogenesis have been studied extensively and a network of essential secreted signaling molecules and downstream transcription factors have been identified. For example, Shh is produced in the palatal epithelium, and members of the Shh pathway, including membrane receptors *Patched1* (*Ptch1*), *Smoothened* (*Smo*) and transcription factors *Gli1-3* are all expressed in the palatal mesenchyme and epithelium (Rice et al., 2006). Loss or reduced Shh signaling activity has been linked to the pathogenesis of cleft palate, as previous studies have shown that epithelium-derived Shh is a necessary mitogen for mesenchymal tissue proliferation (Mo et al., 1997; Zhang et al., 2002; Rice et al., 2004). Cleft palate has also been ob-

[1]Department of Cell and Developmental Biology, Vanderbilt University Medical Center, Nashville, Tennessee
[2]Department of Otolaryngology, Vanderbilt University Medical Center, Nashville, Tennessee
[†]Drs. Huang and Goudy contributed equally to this work.
***Correspondence to: Chin Chiang, Department of Cell and Developmental Biology, Vanderbilt University Medical Center, 4114 MRB3, Nashville, TN 37232. E-mail: chin.chiang@vanderbilt.edu**

DOI 10.1002/dvdy.21714
Published online 19 September 2008 in Wiley InterScience (www.interscience.wiley.com).

served in human patients harboring *SHH* mutations (Nanni et al., 1999). However, there is emerging evidence that excessive Shh pathway activity may also be a cause of palate clefting. First, our recent study of *ShhN/+* mutant mice, which exhibited Shh gain-of-function in many developmental contexts such as in the limb bud, telencephalon, and spinal cord (Li et al., 2006; Huang et al., 2007; data not shown), suggested that cleft palate may arise on ectopic long-range Shh action. Second, recent investigation of *Insig1* and *Insig2* mutants also postulated that excessive Shh may lead to cleft palate (Engelking et al., 2006). Third, it has been reported that a human patient with mutational duplication of distal chromosome 7q, which contains the *SHH* gene locus, displayed cleft palate (Morava et al., 2003). Last, approximately 5% of Gorlin syndrome patients with *PTCH1* mutations, in which Shh pathway activity is elevated, develop cleft palate (Evans et al., 1993). As Gli3 is cleaved into a potent transcriptional repressor in the absence of Shh function, while being an activator in the presence of Shh signaling (Wang et al., 2000; Litingtung et al., 2002), it is of interest to determine what role, if any, Gli3 plays during palatogenesis. Here, we found that Gli3 function does not appear to be essential for autonomous palatal growth, but is likely critical for normal development and proper positioning of the tongue, which is required for palatal shelf elevation and fusion.

RESULTS AND DISCUSSION

Neonatal *Gli3*$^{-/-}$ Mice in the C57/BL6 Genetic Background Exhibit High Incidence of Cleft Secondary Palate

We intercrossed *Gli3*$^{+/-}$ mice that have been maintained in the C57/BL6 genetic background to generate *Gli3*$^{-/-}$ pups. Observation of the progenies after birth revealed that some *Gli3*$^{-/-}$ pups suffered from severe abdominal distention due to air accumulation and absence of milk in the stomach (data not shown), both features paralleling complexions of cleft palate. Indeed, we found high occurrence of cleft secondary palate in neonatal *Gli3*$^{-/-}$ pups. A ventral view of the palate region in a wild-type pup with the mandible removed revealed a normally fused palate (Fig. 1A) that separates the nasal and oral cavities. However, a significant fraction of *Gli3*$^{-/-}$ pups exhibited cleft palates (Fig. 1A′), allowing direct view of the nasal septum. Skeletal staining of *Gli3*$^{-/-}$ mutants further revealed the widely-separated palatine shelves and the presphenoid bone (psp) which is normally underneath the fused palatine shelves (compare Fig. 1B with 1B′). The maxillary shelves were also defective and not fully mineralized in *Gli3*$^{-/-}$ pups (asterisks). Interestingly, we found that the incidence of palate clefting in *Gli3*$^{-/-}$ mutants was dependent on the genetic background with strong predominance in the C57/BL6 background (Fig. 1C). We did not observe significant cleft palate phenotype in *Gli3*$^{-/-}$ mutants that contained mixed backgrounds of CD1, C3H and C57BL6 (data not shown).

To investigate the potential role of Gli3 during palatogenesis, we first analyzed the expression pattern of *Gli3* by radioactive *in situ* hybridization. Because previous studies have shown that there may be intrinsic differences in the development of anterior and posterior palatal shelves (Zhang et al., 2002; Alappat et al., 2005), we analyzed *Gli3* gene expression patterns in both regions. At E13.5, a stage when the palatal shelves are vertically present parallel to the lateral surface of the tongue, *Gli3* expression was prominent in both mesenchymal and epithelial tissues of the palatal shelves (Fig. 1D,D′,E,E′). At E14.0, *Gli3* was expressed in anterior and posterior palatal epithelial tissues facing both oral and nasal cavities, as well as in the mesenchymal tissue close to the fusing midline region (Fig. 1F,F′,G,G′). Furthermore, *Gli3* expression was also prominent in the epithelial and mesenchymal compartments of the developing tongue (Fig. 1D–G,D′–G′).

Gli3$^{-/-}$ Mutant Palatal Shelves Fail to Elevate at Mid-gestation

To determine the onset of morphological palatal defect in *Gli3*$^{-/-}$ mutants, we compared hematoxylin & eosin-stained coronal sections of wild-type and *Gli3*$^{-/-}$ mutant palatal regions, through both anterior and posterior, during key stages of palatogenesis. The palatal shelves first appear with defined shape at around E12.5 and rapidly grow in a vertical plane parallel to the tongue until E13.5 and we observed comparable palatal morphology and development between wild-type and *Gli3*$^{-/-}$ mutants (Fig. 2A,A′,C,C′, data not shown). Between E13.5 and E14.0, while wild-type palatal shelves were positioned in a horizontal plane above the flattened tongue (Fig. 2B,B′), *Gli3*$^{-/-}$ mutant palatal shelves were improperly maintained in a vertical position flanking the protruding, misshapen tongue (arrows in Fig. 2D,D′), however, the size of *Gli3*$^{-/-}$ palatal shelves were comparable to wild-type (Fig. 2D,D′). At E15.5, the wild-type palatal shelves showed contact with significant disappearance of the MES (Fig. 2E), as indicated by loss of epithelial marker, E-cadherin (Fig. 2F). In contrast, most of the *Gli3*$^{-/-}$ mutant palatal shelves had elevated but remain unfused, leaving a wide gap between the otherwise separated nasal and oral cavities (Fig. 2E′,E″). In one severe case, the *Gli3*$^{-/-}$ mutant palatal shelves failed to elevate even at E15.5 (Fig. 2E‴). In all *Gli3*$^{-/-}$ mutants examined, the developmentally defective tongues were consistently tilted, misshapen and more protruding compared with the flattened tongues of wild-type embryos. E-cadherin expression persisted in the unfused midline palatal region of *Gli3*$^{-/-}$ mutants (Fig. 2F′). These results demonstrate a severe delay in palatal shelf elevation in *Gli3*$^{-/-}$ mutants accompanied by defective tongue development. As *Gli3*$^{-/-}$ mutant palatal shelf size was comparable with wild-type, we suggest that the elevation failure is the major cause of palate clefting.

Gli3$^{-/-}$ Mutant Palatal Shelves Do Not Show Alterations in Proliferation or Apoptosis

It has been shown that cell proliferation is an intrinsic driving force for prompt palatal shelf elevation, as loss of *Osr2*, which encodes a zinc-finger transcription factor that is essential

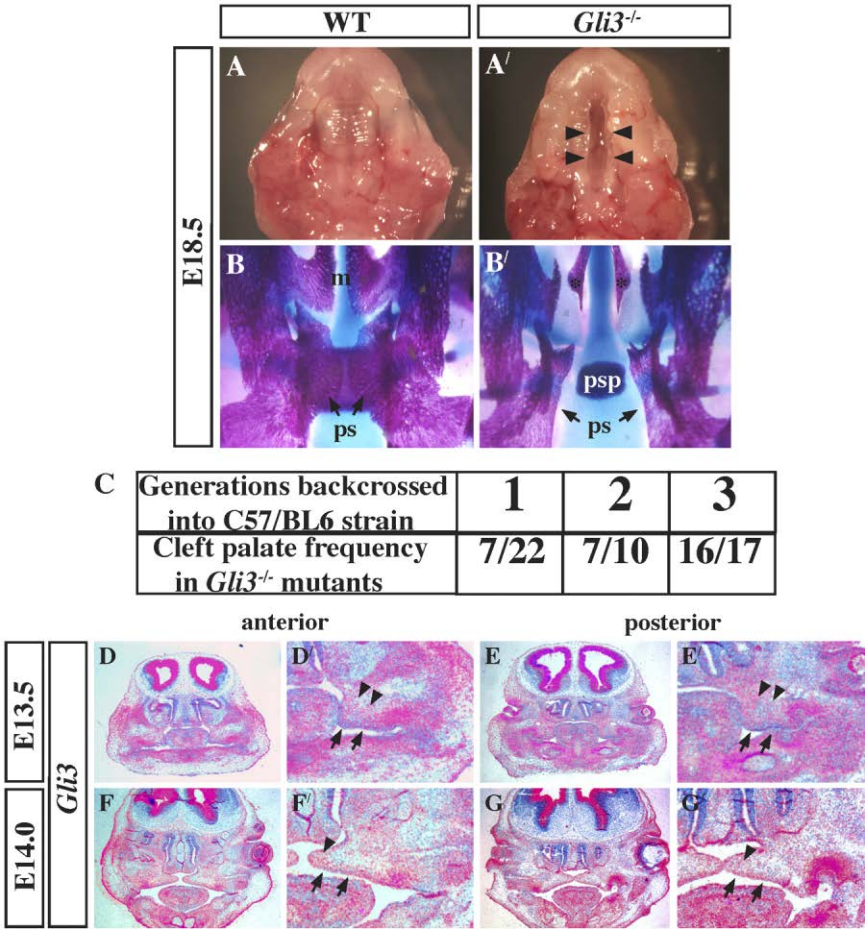

Fig. 1.

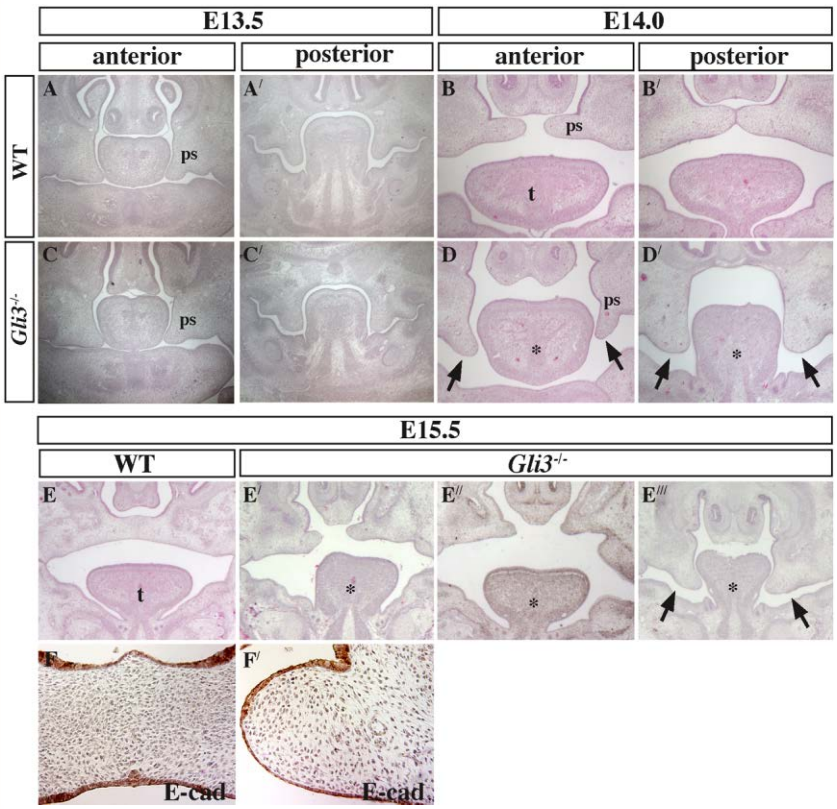

Fig. 2.

for promoting medial palatal shelf proliferation (Lan et al., 2004), led to retardation in palatal shelf elevation and cleft secondary palate. Therefore, we set out to examine whether defective cell proliferation underlies the palatal shelf elevation defect in *Gli3*$^{-/-}$ mutants. We performed 5-bromodeoxyuridine (BrdU) *in vivo* labeling in wild-type and *Gli3*$^{-/-}$ mutants to determine the proliferative capacity of palatal regions. From the initial palatal shelf outgrowth at E12.5 to the completion of palatal el-

Fig. 1. A,A′,B,B′,C: *Gli3*$^{-/-}$ mutant develops cleft palate in C57/BL6 genetic background. **A,A′:** Ventral view of the embryonic day (E) 18.5 wild-type embryo and *Gli3*$^{-/-}$ mutant palatal region with mandible removed. Note wide cleft in *Gli3*$^{-/-}$ mutant, allowing direct view of the nasal cavity. **B,B′:** Skeletal preparation of E18.5 wild-type embryo and *Gli3*$^{-/-}$ mutant palates. Unlike normally closed palatine shelves (ps) in wild-type, palatine shelves are widely-separated in *Gli3*$^{-/-}$ mutants, allowing direct view of underlying presphenoid bone (psp). Note that the bony elements of maxillary shelves (m) are also defective and not fully mineralized in the mutant (asterisks). **C:** Cleft palate frequency in *Gli3*$^{-/-}$ mutants of different generations backcrossed to *C57/BL* background. D,D′,E,E′,F, F′,G,G′: *Gli3* expression pattern during palatogenesis. **D–G:** *Gli3* is widely expressed in many places, including forebrain neuropithelium, nasal septums, tongue, mandibular mesenchyme, perichondrium of Meckel's cartilage and palatal shelves. **D′,E′,F′,G′:** High magnification view showing abundant *Gli3* expression in palatal mesenchyme and epithelium.

Fig. 2. **A,A′,C,C′:** Morphological defects of *Gli3*$^{-/-}$ mutant palate hematoxylin–eosin (H&E) -stained embryonic day (E) 13.5 wild-type and *Gli3*$^{-/-}$ mutant coronal sections through palate region. Comparable-sized palatal shelves grow vertically parallel to the tongue. There is no apparent histological difference. **B,B′,D,D′:** H&E-stained E14.0 wild-type and *Gli3*$^{-/-}$ mutant coronal sections through palate region. At this stage, wild-type palate elevates in a horizontal position above the flattened tongue, however, palatal shelves in *Gli3*$^{-/-}$ mutant remain in a vertical position flanking the tongue similar to E13.5, indicating a delay in elevation. Note that, despite the elevation defect, palatal shelves from either genotype are of similar size. **E,E′,E″,E‴:** Compared with the fused palate in wild-type (E), *Gli3*$^{-/-}$ mutant palatal shelves elevate at E15.5, but fail to meet in the midline (E′,E″), in most severe cases, *Gli3*$^{-/-}$ mutant palatal shelves still remain flanking the tongue (E‴). **F,F′:** Accordingly, epithelial marker E-cadherin disappears in the fused midline palatal tissue (F), while E-cadherin expression persists in the unfused midline palatal tissue in *Gli3*$^{-/-}$ mutant (F′). ps, palatal shelves; t, tongue; asterisks, malformed tongue in *Gli3*$^{-/-}$ mutant.

evation at E14.5, we found no significant proliferative difference in the epithelial or mesenchymal compartment of wild-type and *Gli3*$^{-/-}$ mutant palatal shelves (Fig. 3A,A′,B,B′,C,C′, D,D′,I,J). We confirmed this observation by immunolabeling the phosphorylated form of histone3, an indicator of cells in M phase (Fig. 3E,E′,F,F′, data now shown). We also examined tissue apoptosis in wild-type and *Gli3*$^{-/-}$ mutant palatal regions by TUNEL assay. As previously reported, apparent apoptosis was observed throughout the anterior and posterior MES of the fusing wild-type palate at E14.5 (Fig. 3G,H; Cuervo et al., 2002; Cuervo and Covarrubias, 2004; Murray et al., 2007). We rarely observed apoptotic activity in the anterior palatal shelves of *Gli3*$^{-/-}$ mutants, indicating that the apoptotic event is triggered by palatal shelf contact in this segment (Fig. 3G′). In contrast, apoptosis occurred in both the midline epithelial and adjacent mesenchymal cells in *Gli3*$^{-/-}$ mutant posterior palatal shelves, as in wild-type (Fig. 3H,H′), an observation consistent with a previous report that some periderm cells undergo apoptosis before palatal shelves contact each other to facilitate adhesion (Murray et al., 2007). In all the *Gli3*$^{-/-}$ mutants analyzed (n = 3 for each stage, from E12.5 to E14.5), we did not detect extensive apoptosis that could potentially account for defective palatal elevation. Indeed, there was hardly any cell death in both wild-type and *Gli3*$^{-/-}$ mutants before E14.5 (data not shown). Our findings indicate that neither aberrant proliferation nor apoptosis is likely the underlying cellular mechanism of palate clefting in *Gli3*$^{-/-}$ mutants.

Major Signaling Pathways Regulating Palatogenesis Are Unaffected in *Gli3*$^{-/-}$ Mutants

Because abrogating Shh signaling is associated with cleft palate formation, and Gli3 protein activities are regulated by Shh pathway activity, we first asked whether Shh expression or signaling was altered in *Gli3*$^{-/-}$ mutants. At E13.5, Shh expression was comparable in *Gli3*$^{-/-}$ mutant palatal epithelial tissue and wild-type (Fig. 4A,A′,B,B′). We found that although *Gli3* is robustly expressed in both palatal epithelial and mesenchymal tissue, loss of *Gli3* appeared to have no effect on Shh signaling, as shown by comparable expression of *Ptch1* (Fig. 4C,C′,D,D′), a readout of Shh signaling activity. In fact, overlapping expression patterns of *Ptch1* and *Gli3* in the palate suggested that Gli3 protein might be maintained as full-length activator in this context (compare Fig. 1D,E with Fig. 4C,D). It has been shown that *Msx1* function in the anterior palatal mesenchyme is required to maintain *Bmp4* expression which in turn maintains *Shh* expression in the epithelial tissue. Consistent with normal *Shh* expression in *Gli3*$^{-/-}$ mutants, *Bmp4* and *Msx1* expression appeared unaltered (Fig. 4E,E′,F,F′,G,G′,H,H′). A recent study has shown that Shh expression is also induced by mesenchymal *Fgf10* (Rice et al., 2004). We found that the expression patterns of *Fgf10*, and potential target gene of the Fgf pathway, *Sprouty2*, were also comparable between wild-type and *Gli3*$^{-/-}$ mutants (Fig. 4I,I′,J,J′,K,K′,L,L′). Since disturbances in these signaling pathways have been shown to cause defective palatal tissue proliferation (Zhang et al., 2002; Rice et al., 2004; Alappat et al., 2005), the above data are consistent with our observation that *Gli3*$^{-/-}$ mutant palate proliferation was comparable with wild-type, thus ruling out a proliferation defect as an underlying cause of cleft palate in *Gli3*$^{-/-}$ mutants. The Tgfβ signaling pathway has also been shown to be pivotal for multiple aspects of palatogenesis including CNC-derived palatal tissue proliferation, MES apoptosis and midline epithelial–mesenchymal transition (EMT; Fitzpatrick et al., 1990; Kaartinen et al., 1995; Ito et al., 2003; Nawshad and Hay, 2003). We determined that members of the Tgfβ superfamily, *Tgfβ1* and *Tgfβ3*, were expressed predominantly in the medial epithelial stream and were comparable in wild-type and *Gli3*$^{-/-}$ mutant palates (Fig. 4M,M′,N,N′,O,O′,P,P′). Therefore, our findings indicate that major signaling pathways that regulate palatogenesis are strikingly unaffected in *Gli3*$^{-/-}$ mutant palates.

Cranial Neural Crest Migration Into Palatal Shelves Is Normal in *Gli3*$^{-/-}$ Mutants

We further asked whether the migration of cranial neural crest (CNC), the multipotent progenitor cells that populate palatal tissue, was affected in the absence of Gli3 function. At E10.5, the expression pattern of Ap2 alpha, a CNC migration marker (Mitchell et al., 1991), was comparable between wild-type and *Gli3*$^{-/-}$ mutants (data not shown). Consistently, the distribution of CNC derivatives in the palatal shelf mesenchyme at E10.5 and E13.5 was also comparable (Fig. 4Q,Q′,R,R′,S,S′), as indicated by the *Wnt1cre;R26R* reporter strain. Therefore, we conclude that CNC migration into palatal shelves is normal in *Gli3*$^{-/-}$ mutant and is not the underlying cause of palate clefting.

Gli3$^{-/-}$ Mutant Palatal Shelves Fuse When Cultured Without Tongue

We observed consistent correlation between the cleft palate phenotype and tongue abnormality in *Gli3*$^{-/-}$ mutants (Fig. 2). While there was no distinguishable difference in tongue growth between wild-type embryos and *Gli3*$^{-/-}$ mutants at E13.5, *Gli3*$^{-/-}$ tongues were often misshapen, tilted, and failed to descend after E13.5 (Fig. 2), during which palatal shelf elevation occurs (reviewed in Stanier and Moore, 2004). We propose that abnormal tongue morphogenesis in *Gli3*$^{-/-}$ mutant may impede palatal elevation eventually leading to palate clefting. Because rapid extension of the mandible has been suggested as a physical force driving the forward movement and subsequent lowering of the tongue (Diewert, 1981), a protruding tongue phenotype is generally seen in association with retarded mandibular growth. Thus, we performed cartilage staining to compare the length of the Meckel's cartilage (MC), an embryonic cartilage structure that supports and directs mandibular growth, in wild-type and *Gli3*$^{-/-}$ mutants. However, we found no significant difference in MC lengths (Fig. 5A,A′,B,B′,C,C′,D). Thus, we propose that the cleft palate

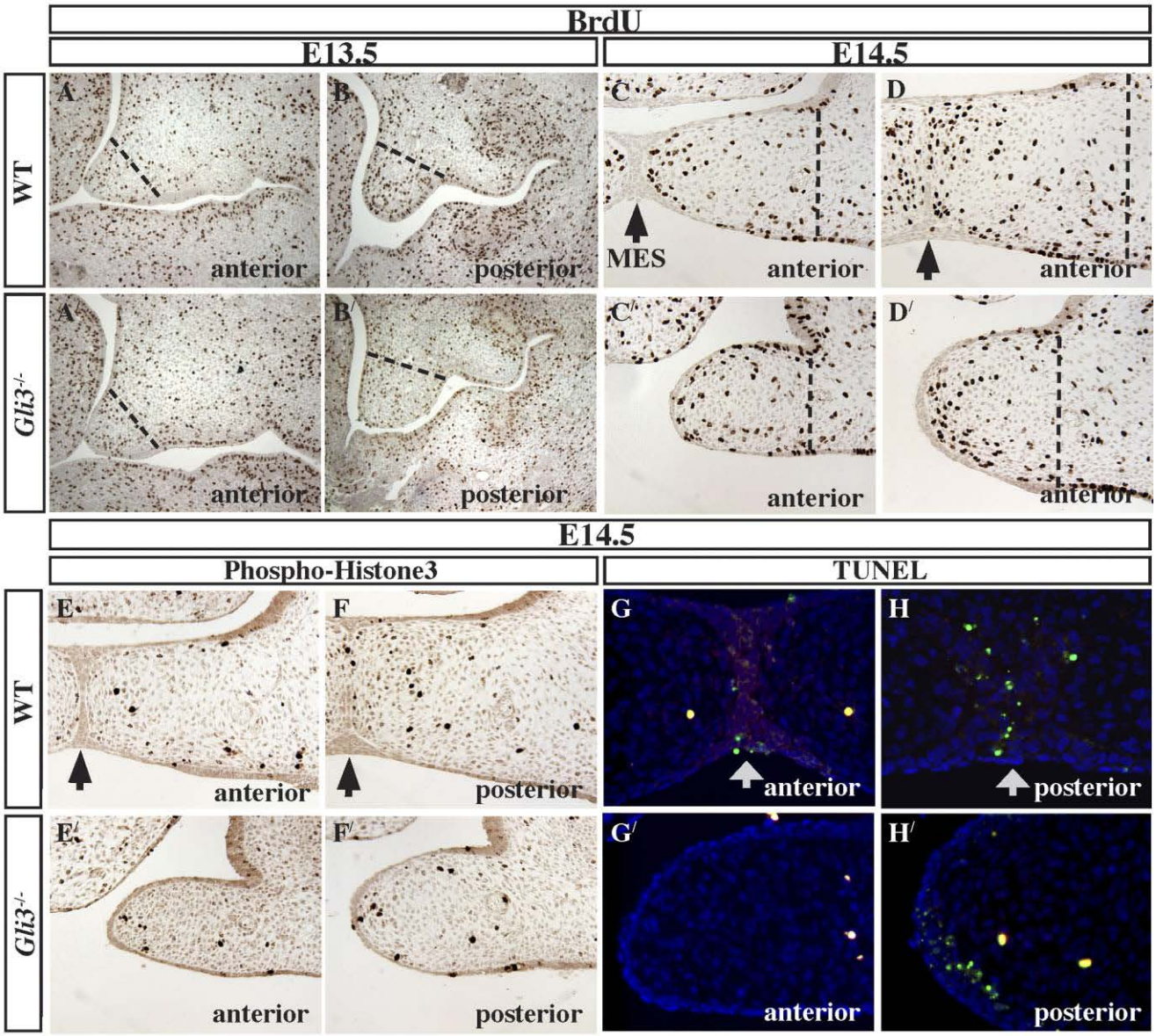

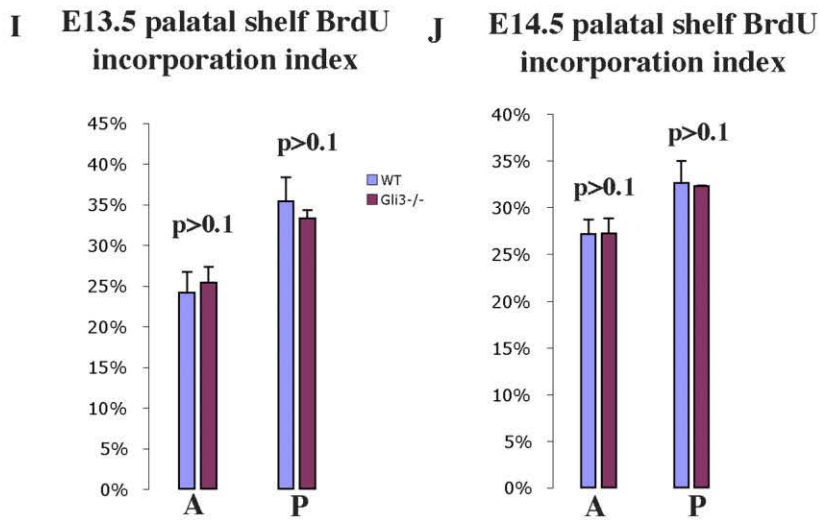

Fig. 3. Proliferation and apoptosis analyses during palatogenesis in *Gli3*$^{-/-}$ mutant. **A,A′,B,B′,C,C′,D,D′,I,J:** 5-bromodeoxyuridine (BrdU) labeling of embryonic day (E) 13.5 and E14.5 wild-type and *Gli3*$^{-/-}$ mutant palates, which display similar proliferation index (I,J). Broken black lines indicate the regions chosen for counting BrdU-positive cells and proliferation index was calculated as percentage of BrdU-positive cells divided by total cell numbers. **E,E′,F,F′:** Phosphorylated form of histone3 labeling also shows similar proliferation pattern between wild-type and *Gli3*$^{-/-}$ mutant palates. **G,G′,H,H′:** Terminal deoxynucleotidyl transferase–mediated deoxyuridinetriphosphate nick end-labeling (TUNEL) analysis reveals apparent cell death in *Gli3*$^{-/-}$ mutant palate.

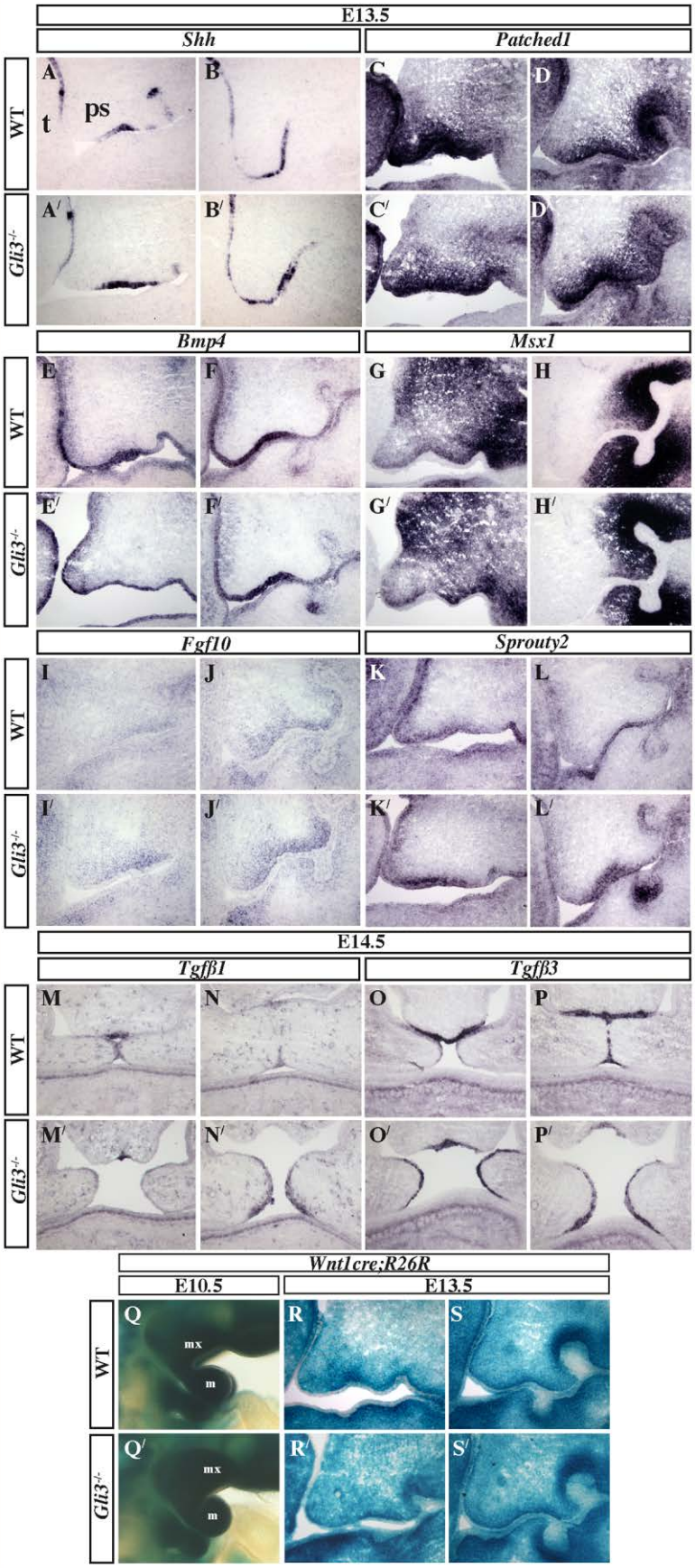

Fig. 4. Major signaling pathways regulating palatogenesis and cranial neural crest (CNC) migrations appear to be unaffected in *Gli3*$^{-/-}$ mutant palate. A,A′,B,B′,C, C′,D,D′: *Shh* and *Ptch1* expression in embryonic day (E) 13.5 anterior and posterior palate. **A,A′,B,B′:** *Shh* expression is similarly confined to epithelium of wild-type and *Gli3*$^{-/-}$ mutant palatal shelves. **C,C′,D,D′:** Correspondingly, strong *Ptch1* expression detected in both epithelial and mesenchymal palatal tissue. **E,E′,F,F′,G, G′,H,H′:** *Bmp4* and *Msx1* expression in E13.5 anterior and posterior palate. *Bmp4* expression is similarly found in the palatal shelf epithelium and adjacent mesenchymal tissue (E,E′,F,F′), *Msx1* expression patterns are also comparable between wild-type and *Gli3*$^{-/-}$ mutant palates (G,G′,H,H′). **I,I′,J,J′,K,K′,L,L′:** Palatal mesenchymal expressions of *Fgf10*, as well as epithelial expression of *Sprouty2* are comparable between wild-type (I,I′,J,J′) and *Gli3*$^{-/-}$ mutant (K,K′,L,L′). **M,M′,N, N′,O,O′,P,P′:** *Tgfβ1* and *Tgfβ3* expression in E14.5 wild-type and *Gli3*$^{-/-}$ mutant palates are also comparable, with strong expression in the midline epithelial tissue. **Q,Q′,R,R′,S,S′:** CNC migrations is unaltered in *Gli3*$^{-/-}$ mutant palate, as evidenced by comparable expression pattern of beta-galactosidase staining of E10.5 and E13.5 wild-type and *Gli3*$^{-/-}$ mutant palatal sections in *Wnt1cre;R26R* reporter background.

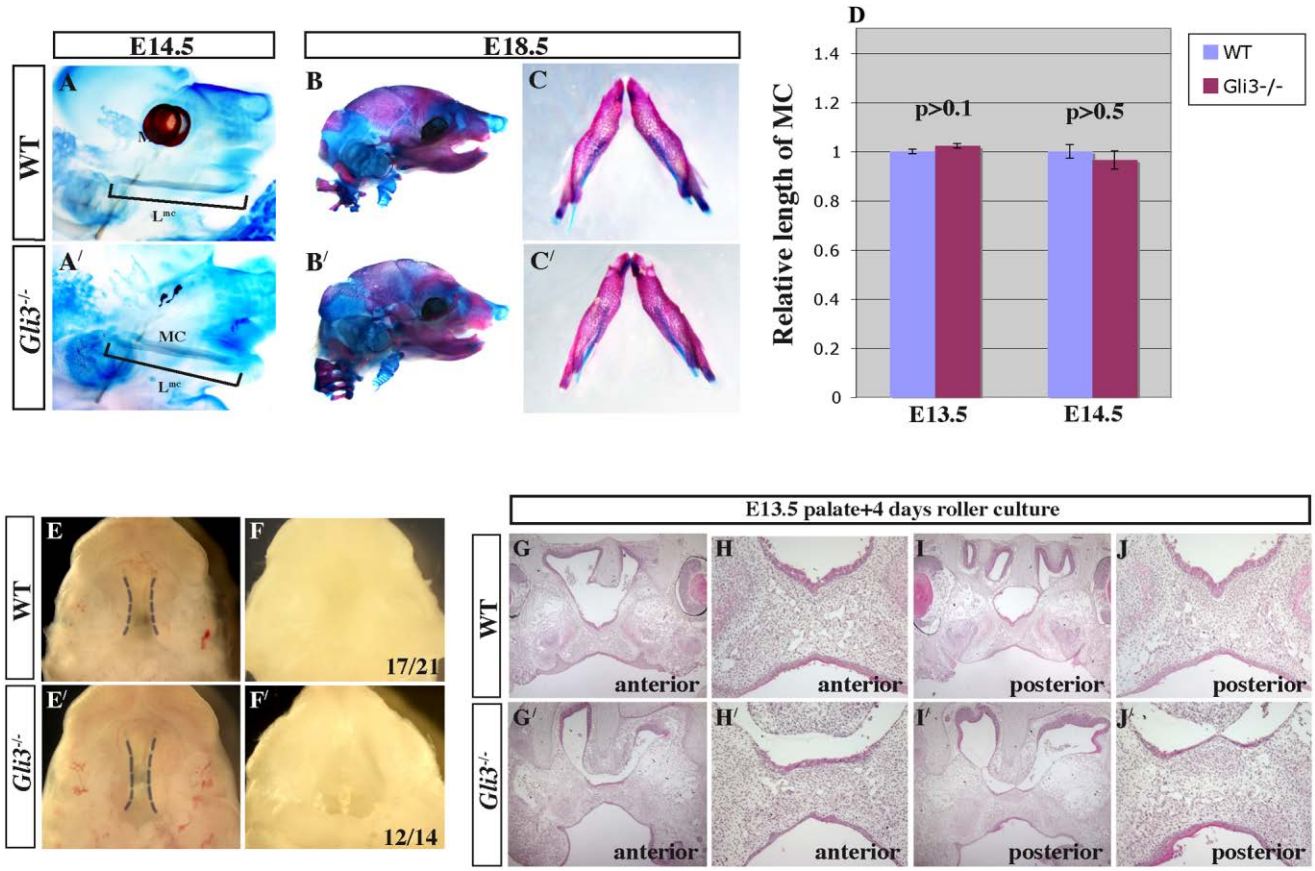

Fig. 5. **A,A′,B,B′,C,C′:** Meckel's cartilage and mandibular skeletal structures develop normally in *Gli3*$^{-/-}$ mutant. At embryonic day (E) 14.5 and E18.5, *Gli3*$^{-/-}$ mutant displays relatively normal MC (A,A′) and mandibular (B,B′ C,C′) skeletal structures. **D:** Absolute length of MC is not significantly different from that of wild-type embryos. E,E′–J,J′: Dissected wild-type embryo and *Gli3*$^{-/-}$ mutant palatal shelves without tongue and mandible are capable of fusing after 4 days of roller culture. **E,E′:** Examples of freshly dissected E13.5 wild-type and *Gli3*$^{-/-}$ palatal shelves. **F,F′:** Examples of wild-type and *Gli3*$^{-/-}$ palatal shelves after 4 days roller culture. **G–J,G′–J′:** Hematoxylin–eosin (H&E) -stained coronal sections of cultured palates shown in E and E′. Note that both wild-type and *Gli3*$^{-/-}$ mutant palatal shelves meet in the midline with complete disappearance of medial epithelial stream.

phenotype in *Gli3*$^{-/-}$ mutant is not associated with defective mandibular growth, but likely due to abnormal tongue development. In agreement, E13.5 wild-type and *Gli3*$^{-/-}$ mutant palatal shelves, grown in roller culture with tongue removed and without added serum or growth factors (Fig. 5E,E′), indicated that mutant palatal shelves can fuse. After 2 days of culture, most *Gli3*$^{-/-}$ mutant palatal shelves were able to join as in wild-type (data not shown). After 4 days, most *Gli3*$^{-/-}$ mutant palatal shelves (12/14, 85%) underwent complete fusion similar to wild-type (17/21, 81%; Fig. 5F,F′). Hematoxylin–eosin stained coronal sections revealed that there were no residual midline epithelial cells in both wild-type and *Gli3*$^{-/-}$ mutant cultured palates (Fig. 5G,G′,H,H′,I,I′,J,J′), indicating that there is no intrinsic growth defect in *Gli3*$^{-/-}$ mutant palatal shelves. This finding supports the notion that defective tongue development may pose an obstruction for palatal fusion in *Gli3*$^{-/-}$ mutants.

In this study, we showed that *Gli3*-deficient mice exhibited genetic background-dependent cleft palate. In mixed backgrounds of CD1, C3H, and C57/BL6, we rarely observed the cleft palate phenotype. In contrast, the penetrance of palate clefting augmented as we backcrossed *Gli3*$^{-/-}$ mutants to C57/BL6. We also showed that, despite its abundant expression in both palatal epithelial and mesenchymal tissue during palatogenesis, Gli3 function is not essential for intrinsic palatal tissue development, as CNC cells appeared to migrate normally into the maxillary prominence of the first pharyngeal arch, and normal proliferation and apoptotic events occurred in *Gli3*$^{-/-}$ mutant palates. Also, Shh, Bmp, Fgf, and Tgfβ pathway activities appeared to be comparable in wild-type and *Gli3*$^{-/-}$ mutants palates. Because *Gli3* expression largely overlaps with those of Shh pathway target genes, such as *Ptch1* and *Gli1* (compare Fig. 1D′,E′ to Fig. 4C,D, data not shown), it is likely that the *Gli3*-expressing domain in this context is a region in which high level of Shh signaling occurs. Thus, Gli3 may mainly function as an activator in palatal tissue. As *Gli1* and *Gli2*, mediators of Shh pathway activity, have been shown to be expressed in palatal shelves (Rice et al., 2006), the potential function of Gli3 in mediating Shh pathway activity may be dispensable in palatal shelf morphogenesis.

It has been proposed that alterations in MC correlated with the

Developmental Dynamics

induction of cleft palate. The administration of lathyrogen beta-aminoproprionitrile (BAPN), a known inhibitor of crosslinking of newly synthesized collagen, at a critical time in secondary palate formation, could induce cleft palate in rats (Diewert, 1981). It has been suggested that inhibition of collagen crosslinking in MC weakens the cartilage during a critical period in facial development when extension of the tongue and mandible beneath the palate are required to facilitate palatal shelf elevation (Diewert, 1981). The requirement for rapid extension of the mandible as a physical force driving forward movement and subsequent lowering of the tongue has also been highlighted by the protruding tongue phenotypes seen in several mouse mutant models with defective mandibular growth, such as *Egfr*$^{-/-}$ (Miettinen et al., 1999), *Hoxa2*$^{-/-}$ (Gendron-Maguire et al., 1993), branchial-specific *dHand*$^{-/-}$ (Yanagisawa et al., 2003), and *Snail1*$^{+/-}$; *Snail2*$^{-/-}$ compound mutants (Murray et al., 2007). However, *Gli3*$^{-/-}$ mutants did not display significant mandibular growth defects, but rather a consistent defect in tongue development. Our finding that the *Gli3*$^{-/-}$ palatal shelves are capable of fusing in the absence of tongue indicates that these mutant shelves do maintain an intrinsic ability to fuse and supports the notion that an abnormal tongue can impede palate formation. *Gli3* is expressed broadly in the developing tongue, including epithelial, mesenchymal and skeletal muscle cells (Fig. 1), thus, the diverse roles that Gli3 might play in the regulation of tongue development remain to be investigated.

EXPERIMENTAL PROCEDURES

Animals

Generation of *Gli3*$^{-/-}$ embryos was carried out by intercrossing *Gli3*$^{+/-}$ mice in the C57/BL6 genetic background. *Wnt1cre* transgenic mice (Jiang et al., 2000) were mated with *R26R-lacZ* reporter strain to study neural crest migration pattern. We used *Gli3*$^{-/-}$ embryos obtained from third generation or higher of C57/BL6 backcrossing for all histological, molecular and culture studies.

Immunohistochemistry

All immunohistochemistry analyses were performed on tissue sections collected from OCT- or paraffin-embedded embryos as previously described (Huang et al., 2007). The primary antibodies were rat anti-E cadherin(ZYMED, 1:100), rabbit anti-phosphorylated histone3 (Upstate, 1:100), and mouse anti-Ap2 alpha (DSHB, 1:100).

Analysis of Cell Proliferation and Apoptosis

The BrdU *in vivo* labeling and terminal deoxynucleotidyl transferase–mediated deoxyuridinetriphosphate nick end-labeling (TUNEL) analysis were performed as previously described (Huang et al., 2007). The percentage of BrdU-positive cells was determined by counting these positive cells in palatal shelf segments within the region designated by broken black lines in Figure 3, divided by the total number of cells in the segment. At least five segments in each region from stainings of three different embryos were counted to generate a statistical comparison. To assess differences among groups, statistical analyses were performed using a one-way analysis of variance (ANOVA) with Microsoft Excel and significance accepted at $P < 0.05$. Results are presented as mean ± SEM.

X-gal Staining and Transcript Detection

X-gal staining for β-galactosidase was performed according to standard protocol. Section in situ hybridizations (digoxigenin-labeled or radioactive) were performed as described (Chiang et al., 1996; Huang et al., 2007). The following cDNAs were used as templates for synthesizing digoxygenin-labeled riboprobes: *Shh*, *Patched1*, *Gli3*, *Bmp4* (S. Lee, Johns Hopkins School of Medicine), *Msx1* (R. Mason, University of North Carolina), *Fgf10*, *Sprouty2* (G. Martin, University of California at San Francisco), *Tgfβ1*, *Tgfβ3* (H. Moses, Vanderbilt University Medical Center).

Cartilage and Skeletal Preparation

Cartilage and bones were stained with Alcian blue and Alizarin red as described (Huang et al., 2007).

Palatal Shelf Roller Culture

Palatal shelf roller cultures were performed essentially according to published methods (Hiranuma et al., 2000). Briefly, E13.5 mouse embryo mid-craniofacial regions were dissected in sterile ice-cold PBS and the brain and lower jaw tissue were carefully removed without damaging the maxillary arch and palatal shelves. Organ cultures were performed in BGJb medium (GIBCO) with penicillin–streptomycin, in a roller culture system infused with 95% oxygen, 5% CO_2 mixture at 37° and at a speed of 25 rpm in a B.T.C. Engineering Precision incubator. It is our experience that grouping palatal shelves together in one 20-ml scintillation glass vial usually yielded better and more consistent culture results. Culture medium was changed at a 24-hr interval and progress in growth, orientation, and fusion of the palatal shelves were monitored. Explants were harvested after 4 days of culture and palatal fusion was compared between wild-type and *Gli3*$^{-/-}$ mutants.

REFERENCES

Alappat SR, Zhang Z, Suzuki K, Zhang X, Liu H, Jiang R, Yamada G, Chen Y. 2005. The cellular and molecular etiology of the cleft secondary palate in Fgf10 mutant mice. Dev Biol 277:102–113.

Chiang C, Litingtung Y, Lee E, Young KE, Corden JL, Westphal H, Beachy PA. 1996. Cyclopia and defective axial patterning in mice lacking Sonic hedgehog gene function. Nature 383:407–413.

Cuervo R, Covarrubias L. 2004. Death is the major fate of medial edge epithelial cells and the cause of basal lamina degradation during palatogenesis. Development 131:15–24.

Cuervo R, Valencia C, Chandraratna RA, Covarrubias L. 2002. Programmed cell death is required for palate shelf fusion and is regulated by retinoic acid. Dev Biol 245:145–156.

Diewert VM. 1981. Correlation between alterations in Meckel's cartilage and induction of cleft palate with beta-aminoproprionitrile in the rat. Teratology 24: 43–52.

Engelking LJ, Evers BM, Richardson JA, Goldstein JL, Brown MS, Liang G. 2006.

Developmental Dynamics

Severe facial clefting in Insig-deficient mouse embryos caused by sterol accumulation and reversed by lovastatin. J Clin Invest 116:2356–2365.

Evans DG, Ladusans EJ, Rimmer S, Burnell LD, Thakker N, Farndon PA. 1993. Complications of the naevoid basal cell carcinoma syndrome: results of a population based study. J Med Genet 30:460–464.

Fitzpatrick DR, Denhez F, Kondaiah P, Akhurst RJ. 1990. Differential expression of TGF beta isoforms in murine palatogenesis. Development 109:585–595.

Gendron-Maguire M, Mallo M, Zhang M, Gridley T. 1993. Hoxa-2 mutant mice exhibit homeotic transformation of skeletal elements derived from cranial neural crest. Cell 75:1317–1331.

Gritli-Linde A. 2007. Molecular control of secondary palate development. Dev Biol 301:309–326.

Hiranuma H, Jikko A, Maeda T, Abe M, Fuchihata H. 2000. Effect of X irradiation on secondary palate development in mice. Radiat Res 154:34–38.

Huang X, Litingtung Y, Chiang C. 2007. Ectopic sonic hedgehog signaling impairs telencephalic dorsal midline development: implication for human holoprosencephaly. Hum Mol Genet 16: 1454–1468.

Ito Y, Yeo JY, Chytil A, Han J, Bringas P Jr, Nakajima A, Shuler CF, Moses HL, Chai Y. 2003. Conditional inactivation of Tgfbr2 in cranial neural crest causes cleft palate and calvaria defects. Development 130:5269–5280.

Jiang X, Rowitch DH, Soriano P, McMahon AP, Sucov HM. 2000. Fate of the mammalian cardiac neural crest. Development 127:1607–1616.

Kaartinen V, Voncken JW, Shuler C, Warburton D, Bu D, Heisterkamp N, Groffen J. 1995. Abnormal lung development and cleft palate in mice lacking TGF-beta 3 indicates defects of epithelial-mesenchymal interaction. Nat Genet 11:415–421.

Lan Y, Ovitt CE, Cho ES, Maltby KM, Wang Q, Jiang R. 2004. Odd-skipped related 2 (Osr2) encodes a key intrinsic regulator of secondary palate growth and morphogenesis. Development 131:3207–3216.

Li Y, Zhang H, Litingtung Y, Chiang C. 2006. Cholesterol modification restricts the spread of Shh gradient in the limb bud. Proc Natl Acad Sci U S A 103:6548–6553.

Litingtung Y, Dahn RD, Li Y, Fallon JF, Chiang C. 2002. Shh and Gli3 are dispensable for limb skeleton formation but regulate digit number and identity. Nature 418:979–983.

Miettinen PJ, Chin JR, Shum L, Slavkin HC, Shuler CF, Derynck R, Werb Z. 1999. Epidermal growth factor receptor function is necessary for normal craniofacial development and palate closure. Nat Genet 22:69–73.

Mitchell PJ, Timmons PM, Hébert JM, Rigby PW, Tjian R. 1991. Transcription factor AP-2 is expressed in neural crest cell lineages during mouse embryogenesis. Genes Dev 5:105–119.

Mo R, Freer AM, Zinyk DL, Crackower MA, Michaud J, Heng HH, Chik KW, Shi XM, Tsui LC, Cheng SH, Joyner AL, Hui C. 1997. Specific and redundant functions of Gli2 and Gli3 zinc finger genes in skeletal patterning and development. Development 124:113–123.

Morava E, Bartsch O, Czakó M, Frensel A, Kalscheuer V, Kárteszi J, Kosztolányi G. 2003. Small inherited terminal duplication of 7q with hydrocephalus, cleft palate, joint contractures, and severe hypotonia. Clin Dysmorphol 12:123–127.

Murray SA, Oram KF, Gridley T. 2007. Multiple functions of Snail family genes during palate development in mice. Development 134:1789–1797.

Nanni L, Ming JE, Bocian M, Steinhaus K, Bianchi DW, Die-Smulders C, Giannotti A, Imaizumi K, Jones KL, Campo MD, Martin RA, Meinecke P, Pierpont ME, Robin NH, Young ID, Roessler E, Muenke M. 1999. The mutational spectrum of the sonic hedgehog gene in holoprosencephaly: SHH mutations cause a significant proportion of autosomal dominant holoprosencephaly. Hum Mol Genet 8:2479–2488.

Nawshad A, Hay ED. 2003. TGFbeta3 signaling activates transcription of the LEF1 gene to induce epithelial mesenchymal transformation during mouse palate development. J Cell Biol 163:1291–1301.

Rice R, Spencer-Dene B, Connor EC, Gritli-Linde A, McMahon AP, Dickson C, Thesleff I, Rice DP. 2004. Disruption of Fgf10/Fgfr2b-coordinated epithelial-mesenchymal interactions causes cleft palate. J Clin Invest 113:1692–1700.

Rice R, Connor E, Rice DP. 2006. Expression patterns of Hedgehog signalling pathway members during mouse palate development. Gene Expr Patterns 6:206–212.

Stanier P, Moore GE. 2004. Genetics of cleft lip and palate: syndromic genes contribute to the incidence of non-syndromic clefts. Hum Mol Genet 13(Spec No 1): R73–R81.

Wang B, Fallon JF, Beachy PA. 2000. Hedgehog-regulated processing of Gli3 produces an anterior/posterior repressor gradient in the developing vertebrate limb. Cell 100:423–434.

Yanagisawa H, Clouthier DE, Richardson JA, Charité J, Olson EN. 2003. Targeted deletion of a branchial arch-specific enhancer reveals a role of dHAND in craniofacial development. Development 130:1069–1078.

Zhang Z, Song Y, Zhao X, Zhang X, Fermin C, Chen Y. 2002. Rescue of cleft palate in Msx1-deficient mice by transgenic Bmp4 reveals a network of BMP and Shh signaling in the regulation of mammalian palatogenesis. Development 129:4135–4146.

Developmental Dynamics